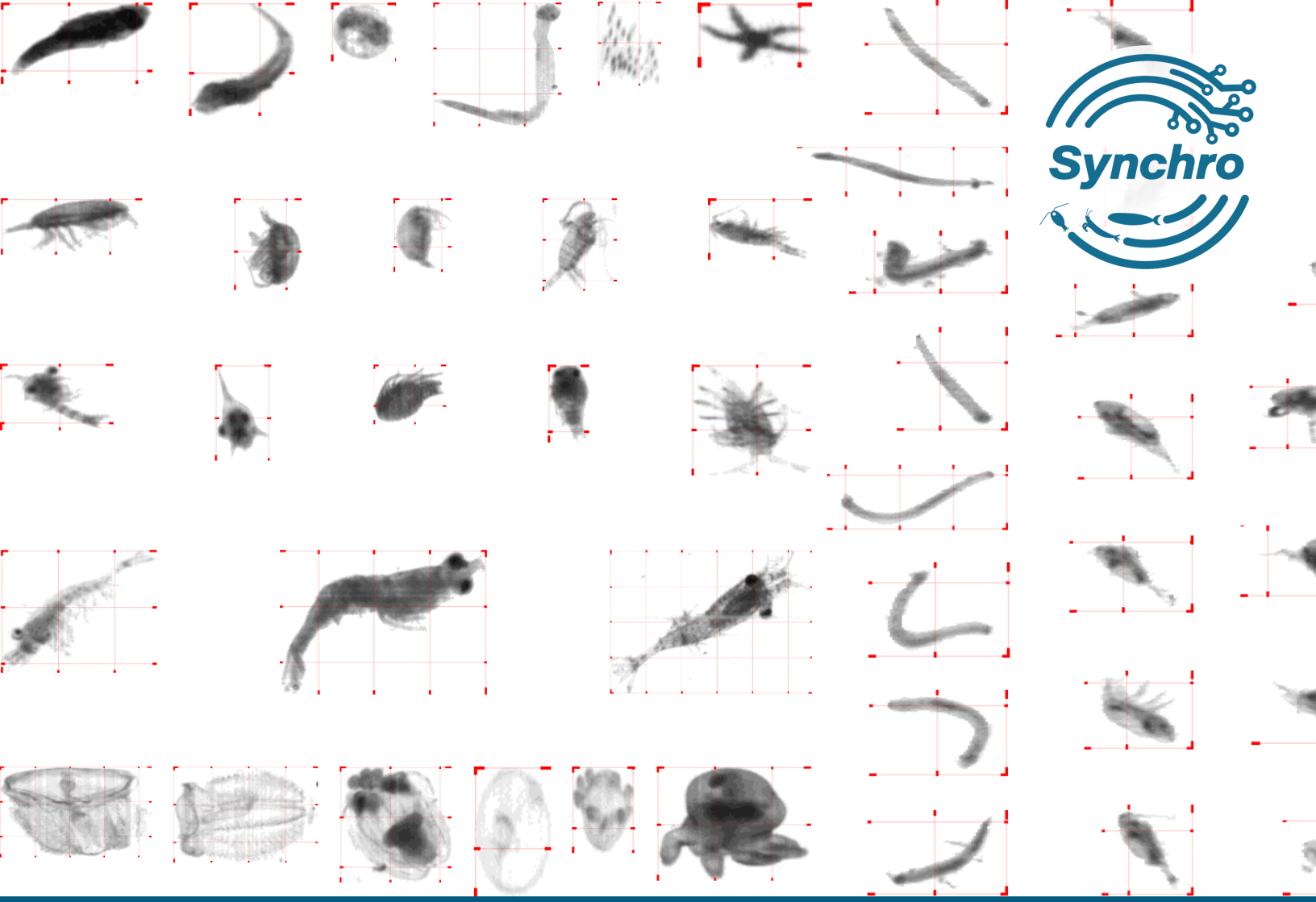

Synchro

Testing & Evaluation Report:

Aquatic Imager: Advancing Zooplankton Classification and Mapping for Ecological Monitoring

OceanSpace
Sensing Solutions for Managing Aquatic Ecosystems

May 2026

OceanSpace Aquatic Imager Test and Evaluation

OceanSpace LLC: Bill Arnold, Kurt Kramer, Milton Dean, Eric Steimle

Synchro: Jason Adelaars, Chamonix Toledo, Henry Ruhl, Amy West

University of California, Santa Cruz: Raphael Kudela, Baldo Marinovic, Kendra Hayashi

Western Flyer Foundation: Katie Thomas

National Oceanic and Atmospheric Administration (NOAA): Andrew Leising

Cal Poly Humboldt University: Eric Bjorkstedt

Point Blue Conservation Science: Jaime Jahncke

Introduction and Background

Scientists and managers from government agencies, academic institutions, and private corporations need more cost-effective and capable means of sampling small particulates such as zooplankton and larval fish (e.g. Lombard et al. 2019, Orenstein et al. 2020). Data on patchily distributed meso- and macro-zooplankton (Robinson et al. 2021), are fundamental to understanding ecosystem status and trends, identifying trophic pathways and (e.g., climate induced) changes to those pathways (Karp et al. 2019), and monitoring patterns of biodiversity and ecosystem services on scales ranging from local to global. Application of such data to management of aquatic ecosystems translates to a more predictable ecosystem capable of reliably delivering essential ecosystem services (Palmer 2017).

To meet this need, OceanSpace LLC has developed the Aquatic Imager, a flow-through optical imaging system featuring a high-speed line-scan camera that obtains high resolution (7 µm pixel size) images of small particulates (e.g., zooplankton, fish larvae, microplastics) in the ~0.5-50 mm size range. Both grayscale and color line-scan camera arrangements are available. The imaging unit is relatively small, lightweight, and rugged (Figure 1), rendering it suitable for use on crewed or uncrewed vessels, shoreside in stream settings, integrated into aquaculture operations, or for processing previously collected samples in the laboratory. The imaging unit is not submersible, thus requiring water to be delivered to the imaging unit via a variety of sample intake options.

Figure 1. Front (top) and back (bottom) views of the Aquatic Imager imaging unit. Front view shows front- and back-light intensity controls and camera access panel. The back view shows computer and auxiliary connectors, power connections, and on-off switch. 1” ID plumbing connection ports are visible on each side of the imaging unit.
Photo: W. Arnold / OceanSpace LLC

For deployment aboard vessels ranging in size from small boats to research vessels, a plankton net or other intake device can be connected via a 1” (2.54 cm) inner diameter hose to the imaging unit (Figure 2). When deployed over the side of a vessel, or for a static deployment such as a dock or pier, water is drawn through the imaging unit by a pump (e.g., centrifugal bilge pump) located distal to the imaging unit. On larger vessels equipped with an in-line seawater system, the imaging unit can be connected directly to the in-line system, with no pump needed; so long as any upstream filtering or pump impellers do not adulterate the feed water going into the imaging unit.

Figure 2. Plankton net intake with hose connector.

The Aquatic Imager uses proprietary software for system operation, training library development, and image classification/enumeration (Bowman et al. 2026). The software is installed on a computer that is hardwired to the imaging unit via a GigE cable. Pixelated data are delivered from the imaging unit to the software, which packages the pixels into individual images and stores those images in a file specific to each sampling event. As images are obtained during a sampling event, a subset of those sampled images is displayed on the computer screen, allowing the user to monitor the images being collected in near-real-time. This facilitates adaptive sampling, in the sense that the image stream may alert the user to an interesting event for which a more focused sampling strategy could be implemented. Following a sampling event, the full suite of images is available for review and classification. Also of note, a time stamp with seconds-scale resolution is assigned to each image, enabling alignment with Geographic Positioning System (GPS) data in support of fine-scale temporal plotting, spatial mapping at the resolution of the GPS unit, and integration with ancillary data such as temperature, salinity, and dissolved oxygen to reveal forces influencing plankton distribution patterns.

The training library is an essential feature of the classification process. A base library, provided with the software package, provides the starting point for library development. However, it’s unlikely the base library will be suitable and sufficient for application to images collected from the user’s specific location. Instead, the user collects a suite of images from their location of interest, then manually assigns a subset of those images to appropriate classes, such as copepods, cladocerans, or chaetognaths. The taxonomic level to which the user can classify an image (the image validation process) depends on factors such as the taxonomic expertise of the user, the morphological characteristics of the organism, and the extent to which morphologically similar but taxonomically distinct organisms are present in the sample. For example, classifying images to the copepoda vs cladocera class may be relatively straightforward, whereas

classifying to copepod genus *Acartia* vs *Temora* could be more difficult and to species within the *Acartia* genus yet more difficult. A strength of the Aquatic Imager is the ability to deliver ecological (e.g., temporal and/or spatial) resolution resulting from the seconds-scale time stamp assigned each image, but there is a tradeoff with taxonomic resolution.

As noted above, each training library is developed by the user for a specific application (e.g., sampling location). This ensures the images included in the library are representative of the location being sampled. When developing a training library, the user reviews image classifications initially assigned by the software using an existing library. Multiple libraries may be available to the user, including the base library and libraries developed by the user for application to specific locations or conditions. The software allows the user to choose the library they wish to use for classification of a specific sample. When developing a library, the user reviews the initial classifications, then re-assigns images among classes as appropriate to improve the model's classification skill to achieve a desired level of classification accuracy for each class, thereby expanding and strengthening the training library. This machine-learning based method of supervised training is another key system feature, enabling rapid user training of image libraries specific to the user's region. Training library development involves an iterative reclassification process. For samples containing only a few distinct taxonomic classes, a training library that delivers classification accuracy exceeding 80% for a specific class may be achieved with only a few iterations of the image validation process. As the number of unique organism classes increases, the number of iterations required to achieve desired classification accuracy for one or more classes likely also will increase. However, once a training library achieving the desired classification accuracy has been built, little if any additional training library work will be required. Instead, the software is now ready to be used on a routine basis to achieve near-real-time classification.

Plankton data are essential to understanding marine ecosystem status broadly, informing indicators ranging from ocean productivity and biodiversity to the forage base that supports fish, seabirds, and marine mammals (Karp et al. 2019). Integrated Ecosystem Assessments (IEAs) represent a formalized framework for translating this monitoring data into actionable management advice, tracking indicators such as northern and southern copepod biomass anomalies and krill (*Euphausia pacifica*) length and biomass as measures of lower trophic level productivity and forage availability, as demonstrated for example by the California Current Integrated Ecosystem Assessment (CCIEA) (NOAA 2025). These indicators are presented annually to the Pacific Fishery Management Council (PFMC), the Regional Fishery Management Organization (RFMO) responsible for setting harvest levels for species including salmon, groundfish, and coastal pelagic species along the U.S. West Coast. The IEA approach extends beyond the California Current Large Marine Ecosystem (CCLME) and is being developed and implemented across Large Marine Ecosystems worldwide, where Regional Fishery Management Organizations similarly depend on ecosystem-level monitoring data to support sustainable fisheries governance.

We tested this novel zooplankton camera for a day on a wharf station and also on a cruise aboard a coastal vessel in Monterey Bay, in the context of potential to inform IEAs and similar

concepts using zooplankton data to inform fisheries quota setting. The primary objective of this technology testing effort was to evaluate the performance of the Aquatic Imager and associated sampling accessories in a shipboard setting. For this test, the grayscale version of the Aquatic Imager was deployed. The grayscale version is well-suited for marine deployments, where most organisms are translucent so color is rarely a diagnostic feature. When these conditions hold, an added advantage of the grayscale version relative to the color version is less pixel-dense images, allowing higher flow rates and less data storage demand. Specifically, we examined the system's capability for addressing the question of what are the taxon / indicator specific concentrations of plankton? And, what are the operational and analytical features considered in producing such data for management applications?

Methods

System testing was conducted by Synchro staff aboard the R/V Western Flyer during a one-day cruise in Monterey Bay, California, on November 12, 2024. For that effort, a 330 µm mesh plankton net, which served as the sample intake, was deployed over the port side of the vessel and connected to the imaging unit via a 1" (2.54 cm) I.D. hose. Water was pushed through the plankton net via forward vessel motion, subsidized by pull from a 6 gallon (23 l) per minute bilge pump located distal to the imaging unit (Figure 3). Following passage through the imaging chamber and the bilge pump, water and organisms flowed over the side of the vessel and into Monterey Bay.

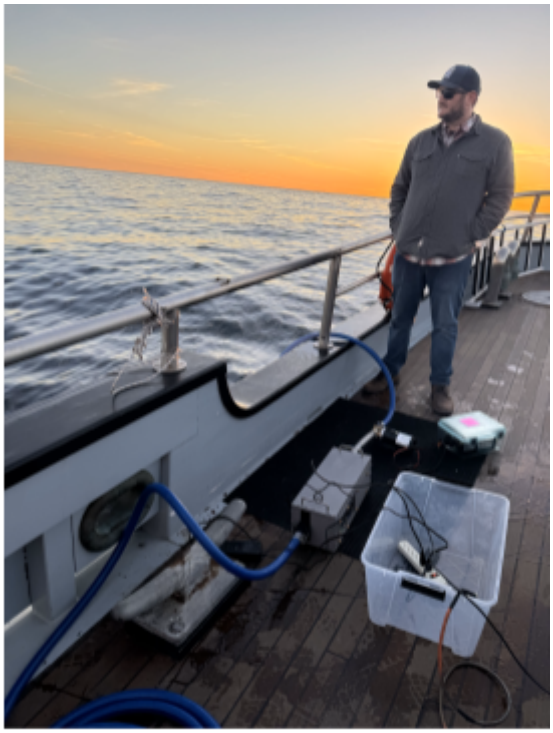

Figure 3. Deployment of the Aquatic Imager from the deck of the R/V Western Flyer in Monterey Bay, California.

Performance evaluation involved deploying the Aquatic Imager on the deck of the R/V Western Flyer in Monterey Bay, collecting a sample by drawing water through a 2.54 cm inner diameter hose deployed over the side of the vessel and through the Aquatic Imager while underway (Figure 3), assigning those images to taxonomic class using the OceanSpace Image Manager software package, and evaluating classification accuracies by application of a confusion matrix analysis described in detail below. Note that the Aquatic Imager works best in a particle range of ~0.5 – 50 mm, although many factors influence the ability of the imager and associated software to collect a suitable image and successfully classify that image to the correct class. Those factors will include for example particle morphology, distinctness relative to other particle classes, front- and back-light settings, and the abundance of the particle class. Also note that the lower limit is determined by optics, whereas the upper limit is determined by

the ability of the particle to pass through the imaging chamber. A particle can be very long, up to ~52 mm high, but no larger than ~9.9 mm wide and still successfully pass through the imaging chamber. However, organisms much larger in every dimension, such as ctenophores, have successfully passed through the imaging chamber.

Evaluations included the physical ability of the sample intake system to deliver water through the imaging unit with the unit positioned on the ship deck, image clarity with respect to class assignment, training library development effort, and classification accuracy within each representative class obtained during the sampling event. An additional consideration was the suitability of the resultant data for meeting data and information needs for Integrated Ecosystem Assessments (IEAs) and similar concepts that use plankton data to inform fisheries quota setting.

Figure 4. Image of bubble obtained during sampling aboard the Western Flyer. Increments are 1 mm.

Image collection evaluation included a consideration of both the effectiveness of the line-scan camera to collect image pixels as particles passed through the imaging chamber and effectiveness of the software to package those pixels into independent images. As discussed above, image classification is an inherent feature of the software. Classification success (i.e., accuracy) depends upon the user's ability to correctly identify organisms to a specific class (lowest possible taxonomic unit) and their ability to use that knowledge to build a representative training library. A representative training library includes, for each class, a large number of images (ideally 1000 or more, although in practice that many images will not be available for every class of organism) in a variety of orientations.

Evaluation of the ability of the system to deliver water to the imaging unit was determined by two separate but independent means. At the coarser scale, was water passing through the system at the desired flow rate? This determination was obvious upon visual inspection, but can be determined quantitatively by measuring the rate at which a known volume container is filled, or more precisely by installing a flow meter into the flow path. At the finer scale, is the water flow smooth and consistent, determined largely by examining the inevitable bubbles that flow through the imaging chamber? This was easily monitored by watching the video screen; bubbles are obvious and apparent (Figure 4). Bubbles are a common feature of water flow, so a complete lack of bubbles is not expected, but if bubbles are passing through the chamber at a density that obscures other particles, this issue must be solved. Causative factors could include position of the mouth of the intake or a leak along the intake path.

Another aspect of water flow is the relationship between the rate of water flow through the imaging chamber and the camera scan rate. These parameters need to be aligned for best image quality. As noted above, best alignment of flow rate with scan rate is achieved by installing a flow meter on the intake hose proximal to the imaging unit. This allows precise determination of flow rate, from which the appropriate scan rate can be determined using the available OceanSpace flow rate/scan rate table. For the Western Flyer deployment (and in

many other deployment settings), a flow meter was not available. An alternative method was instead employed, based on monitoring the 'roundness' of the water bubbles as they are visualized flowing through the imaging chamber. If the bubbles are round, or at least close to being round, a relatively good match has been achieved. A perfect match between flow rate and scan rate is not required to obtain good images, and in fact flow rate will vary during a sampling episode in concordance with variations in vessel forward motion, surface current fluctuations, and other factors.

Evaluation of software-based image classification performance was determined as follows. All images collected during the sampling event were classified (i.e., validated) by OceanSpace principal William Arnold. Accuracy of software-based classification was then evaluated using a confusion matrix routine embedded in the proprietary OceanSpace Image Manager software, which compares the user-validated classifications to classifications determined by the software using the user-developed training library. The output from the confusion matrix operation is a matrix (see Appendix I) comparing classifications based on user validation with classifications based on the Convolutional Neural Network (CNN)-based image classification algorithm that applies knowledge contained in the training library (Ali et al. 2023).

Five metrics were calculated from the confusion matrix output:

1) Accuracy shows how many predictions the model got right out of all of the predictions made by the model.
   Accuracy = (True Positives (TP) + True Negatives (TN))/(TP+TN+False Positives (FP) + False Negatives (FN))

2) Precision shows how many of the model's positive predictions were actually correct.
   Precision = TP/(TP+FP)

3) Recall shows the proportion of true positives detected out of all of the actual positive instances.
   Recall = TP/(TP+FN)
4) F1 Score combines Precision and Recall into a single metric, providing a sense of the model's overall performance.
   F1 Score = (2*(Precision*Recall))/(Precision+Recall)

5) Specificity measures the ability of the model to correctly identify negative instances.
   Specificity = TN/(TN+FP)

Results

The software identified (classified) organism images into three classes from the data obtained during the Monterey Bay sampling event: chaetognaths, cladocerans, and copepods. Representative images of these three classes are included in Appendix II. A fourth, smaller group of images was assigned as unknown because they could not be confidently identified by

the user. Additional (generally inorganic) assignment classes included detritus, bubbles, and noise, assignment classes common to many sampling locations. Relative to other locations, where a wider range of distinct organism classes are commonly encountered (see Appendix III for representative images from other locations), these few organism classes resulted in better classification success (Ali et al. 2023) when compared with classification of samples from Tampa Bay, Florida (Appendix IV). Specifically, the Monterey Bay samples required fewer reclassification events to achieve our targeted classification accuracy of >90%. We consider a software-based classification accuracy ≥ 80% (relative to validated samples, based on confusion matrix outcome) to be good, and a classification accuracy ≥90% to be very good.

Taxon and Indicator Specific Plankton Concentrations

In the case of chaetognaths (Figure 5), for which the organisms are relatively distinct in comparison to cladocerans and copepods, an accuracy exceeding 80% was achieved upon initial classification. For that initial classification, we used as a start point a classification library containing images collected from Tampa Bay, Florida. Then, prior to the first classification run, we added 122 of the 330 validated chaetognath images (37% of the total number of validated images) to the training library. An accuracy exceeding 90% was achieved following a single reclassification that included 158 (48%) of the 330 validated images. Following additional assignment of validated chaetognath images to the training library and subsequent reclassifications, accuracies fluctuated slightly but remained above 90%.

In the case of cladocerans (Figure 6), for which the images are relatively distinct especially in comparison to chaetognaths, initial classification accuracy was only ~47%, with a training library population of 30 of the 177 validated images (17%). This outcome likely reflected morphological similarities between the cladocerans and the copepods. Following a second reclassification, classification accuracy increased substantially, to ~88% with 48 (27% of total validated images) included in the training library. The conflict in classification success between cladocerans and copepods is evidenced by the large percentage (36%) of cladocerans misclassified as copepods following the initial classification event.

Classification outcomes for copepods fell in-between those for chaetognaths and cladocerans (Figure 7). Initial classification accuracy was ~79%, with a training library population of 53 of the 463 validated images (11%). Most misclassified copepod images (~22%) were classified as noise. Following a second reclassification, classification accuracy increased to ~88% with 122 (26% of total validated images) included in the training library. Images classified as noise decreased to <5%.

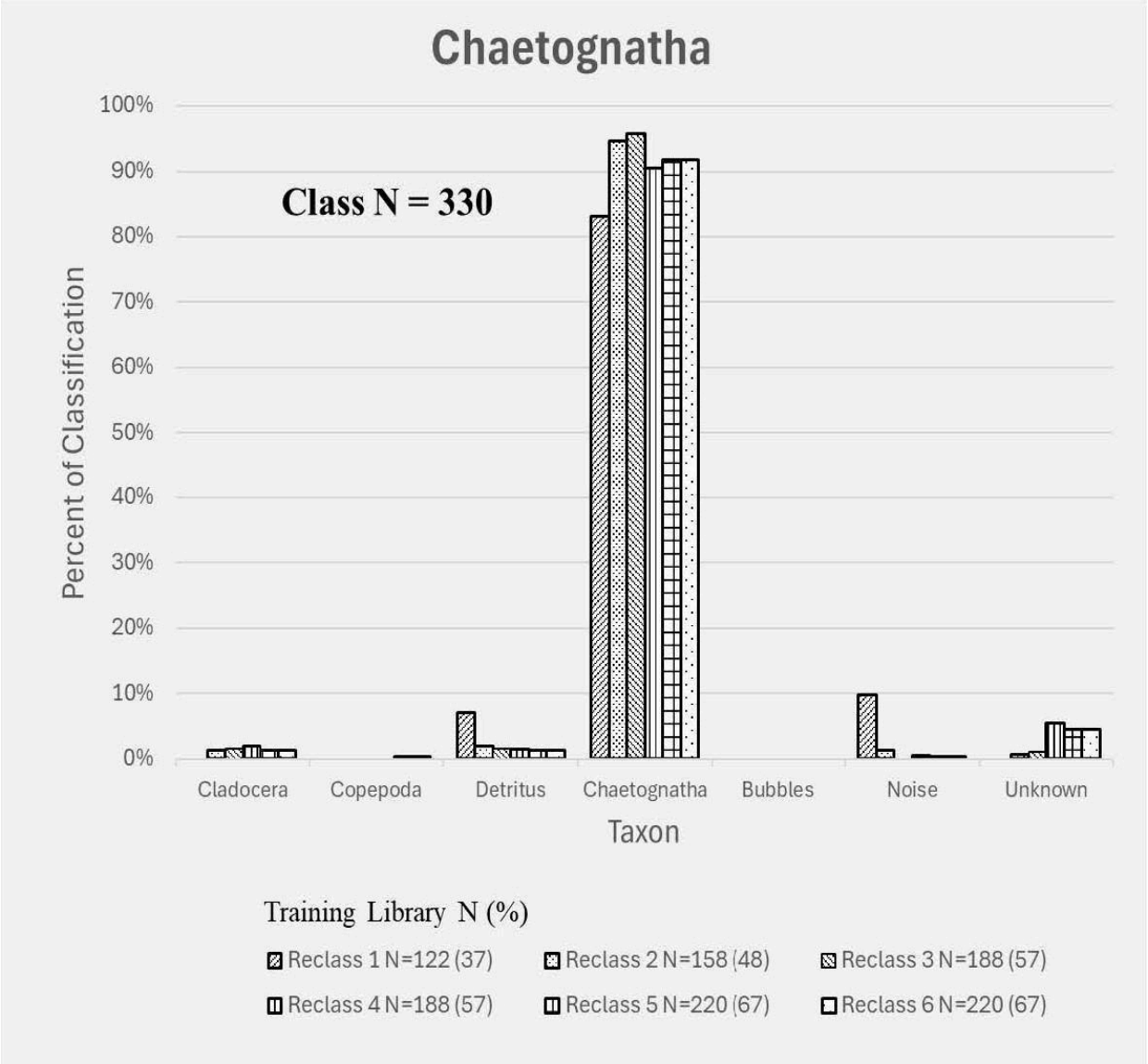

Figure 5. Sequential classification outcomes for chaetognaths collected aboard the R/V Western Flyer during a November 12, 2024, sampling event in Monterey Bay, California. 'Class N' is the total number (330) of chaetognath images validated from the sample. 'Percent of Classification' is the percent of validated chaetognath images that were assigned to each class during each reclassification event. 'Training Library N' is the number of validated chaetognath images included in the training library prior to each reclassification event, with the percent of the total number of validated chaetognath samples presented in parentheses. 'Reclass x' is the reclassification event, of which there were six in total. Thus, Reclass 1 included 122 validated chaetognath images in the training library, representing 37% of the total number of validated chaetognath images. Reclass 1 achieved a classification accuracy of ~83%, meaning that 83% of the validated chaetognath images were correctly assigned to the chaetognath class, and 17% of the validated chaetognath images were incorrectly assigned to the other classes. For Reclass 2, 26 validated chaetognath images were added to the training library, resulting in 158 validated chaetognath images in the training library (48% of the total number of validated chaetognath images). For this reclassification event, ~94% of the validated chaetognath images were correctly assigned to the chaetognath class, and 6% of the validated chaetognath images were incorrectly assigned to the other classes. Data for the other classes follow the same principles and indicate their reclassification outcomes.

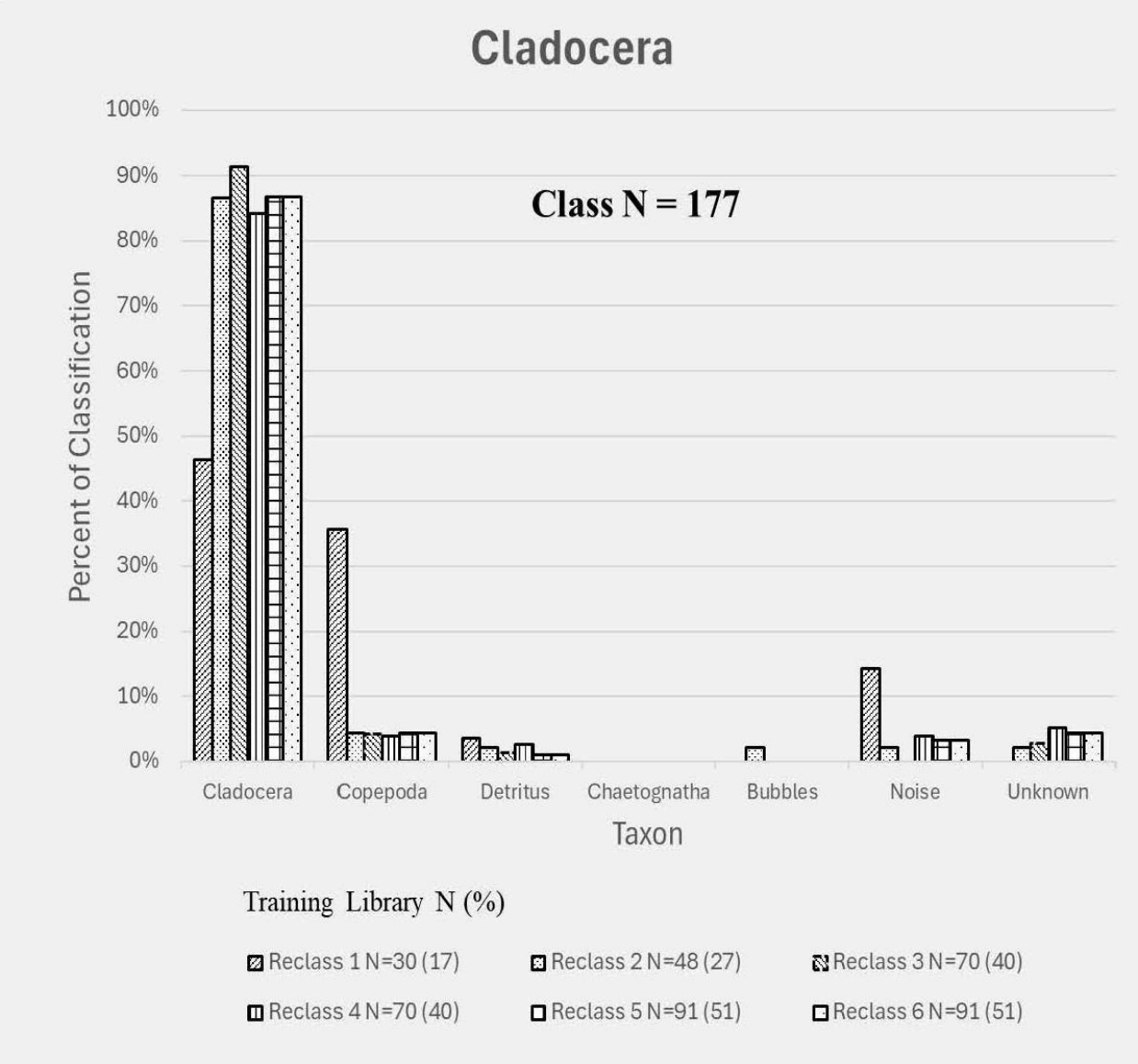

Figure 6. Sequential classification outcomes for cladocerans. Figure description is essentially the same as for Figure 5. In this case, 177 images were validated as cladocerans. Initial classification accuracy was only ~47% based on a training library population of 30 representing 17% of the total number of validated cladoceran images. Classification accuracy increased to ~88% following a second reclassification that included 48 validated cladoceran images (27% of the total number of validated cladoceran images) in the training library. Most misclassified cladocerans (~36%) were classified as copepods following the initial classification, with misclassifications decreasing to ~5% in subsequent reclassifications. No cladocerans were misclassified as chaetognaths, evidence of the morphometric distinction between these two classes.

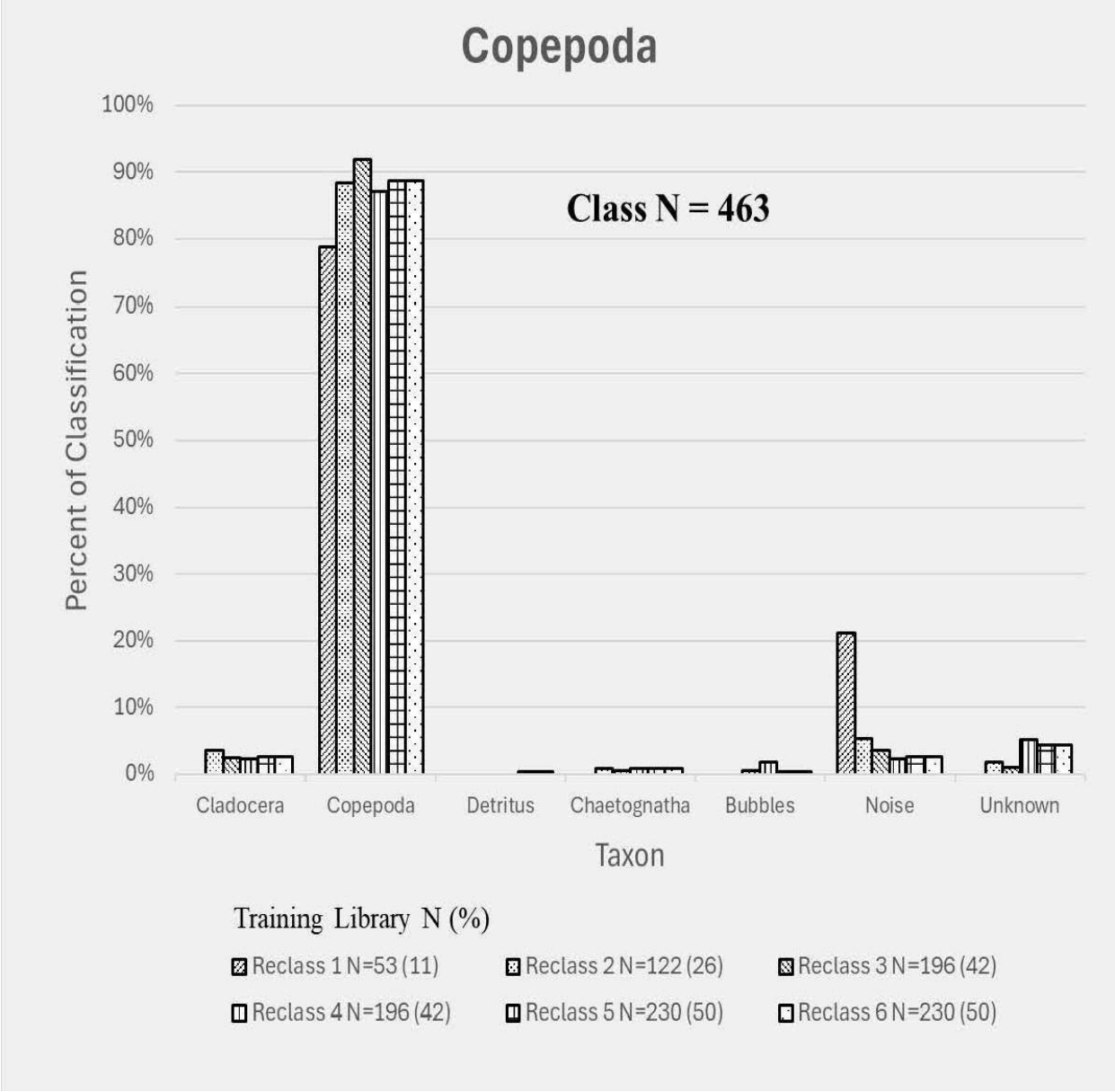

Figure 7. Sequential classification outcomes for copepods. Figure description is essentially the same as for Figure 5. In this case, 463 images were validated as copepods. Initial classification accuracy was ~79% based on a training library population of 53 representing 11% of the total number of validated copepod images. Classification accuracy increased to ~88% following a second reclassification that included 122 validated copepod images (26% of the total number of validated copepod images). Most misclassified copepods (~22%) were classified as noise following the initial classification, with misclassifications to all classes decreasing to <5% in subsequent reclassifications.

Additional parameter values can be calculated based upon knowledge of the volume of water processed during the sampling event. The flow rate of water through the Aquatic Imager, driven by forward vessel motion coupled with pull from the attached pump, was estimated to be 1m/sec. This water was flowing through an imaging chamber with dimensions 1.0 cm width x 5.3 cm height, an area of 5.3 cm^2 (0.00023 m^2). Multiplying flow rate by area returns a flow volume of 0.00053 m^3/s. The length of the sampling episode, determined from the number of scan lines

read (11,193,339) and the scan rate (25,000/sec), was 447 seconds. Thus, the total volume processed during the 447 second sampling event was 0.00053 m^3/s x 447 s = 0.23691 m^3 or 236.91 L. This allows determination of the density of each taxon class in the sample. For chaetognaths, the density was 330 organisms/0.23691 m^3 = 1393 organisms/m^3. Similarly for cladocerans (177 organisms = 747 organisms/m^3) and copepods (463 organisms = 1954 organisms/m^3).

For copepods, the density we report is in reasonable agreement with results reported for the upper 200 m of the Monterey Bay water column during 1997-1999 collected using a 200 micron-mesh plankton net (Hopcroft et al. 2002). Those authors reported a mean abundance of the copepod assemblage of 1267/m^3. However, data on the density of chaetognaths and cladocerans in Monterey Bay were not discovered. Chaetognath density data are largely unavailable in general. Reported cladocera density in a Brazilian coastal lagoon (Rosa et al. 2021) peaked at over 4500/m^3, with a study average of 1799 $\pm$ 3103/m^3.

Applications Discussion

The OceanSpace Aquatic Imager is designed for a wide range of applications, including for example industrial entrainment monitoring, assessing microplastics in aquatic ecosystems, and classifying, enumerating, and mapping freshwater and marine zooplankton in environments ranging from small streams to the open ocean. The imager itself is rugged and water resistant, thus suitable for field deployment, but it is not submersible. Instead, specific accessories are available to deliver water through the system depending on location and environment. As described in the Methods section, the Western Flyer sampling episode utilized a plankton net intake connected to the imager via flexible hose.

Operational and Analytical Features for Management Applications

Based on the single sample collected for this study, and the relatively short duration of the sample collection, only basic inferences regarding applications of the Aquatic Imager technology can be obtained. Those inferences must be considered within the context of a single sample, preventing any estimation of variability among samples or locations. Nonetheless, these results support the contention that the Aquatic Imager does produce data applicable to assessing the status of a key California Current indicator ‘species’ (copepods), and could be similarly useful for assessing the status of other indicators including (but not limited to) krill, fish larvae, and gelatinous organisms. It’s important to note that much longer sample durations are supported by the Aquatic Imager, including continuous sampling aboard the R/V Weatherbird for durations ranging from 15 minutes to several hours. The key constraint is data storage. For the R/V Weatherbird deployments, and for other deployments in a variety of industrial and research settings, a 1 TB storage drive incorporated into the attached laptop computer is sufficient for conduct of multi-hour data collection episodes. An important feature of the software package is the assignment of a seconds-scale time stamp to each image. This enables matching the image

data with concurrently collected Global Positioning System (GPS) coordinate data and thereby plotting the collection point of each image. From that, spatially-resolved maps of the location of each member of a class along the sampling transect can be derived (and overlaid), such as was done for copepod sampling along the southeast coast of Florida using Geographic Information System (GIS) mapping technology (Figure 8). This is a powerful feature of the Aquatic Imager technology. Unfortunately, the GPS unit aboard the R/V Western Flyer was not functioning during the cruise, preventing similar mapping.

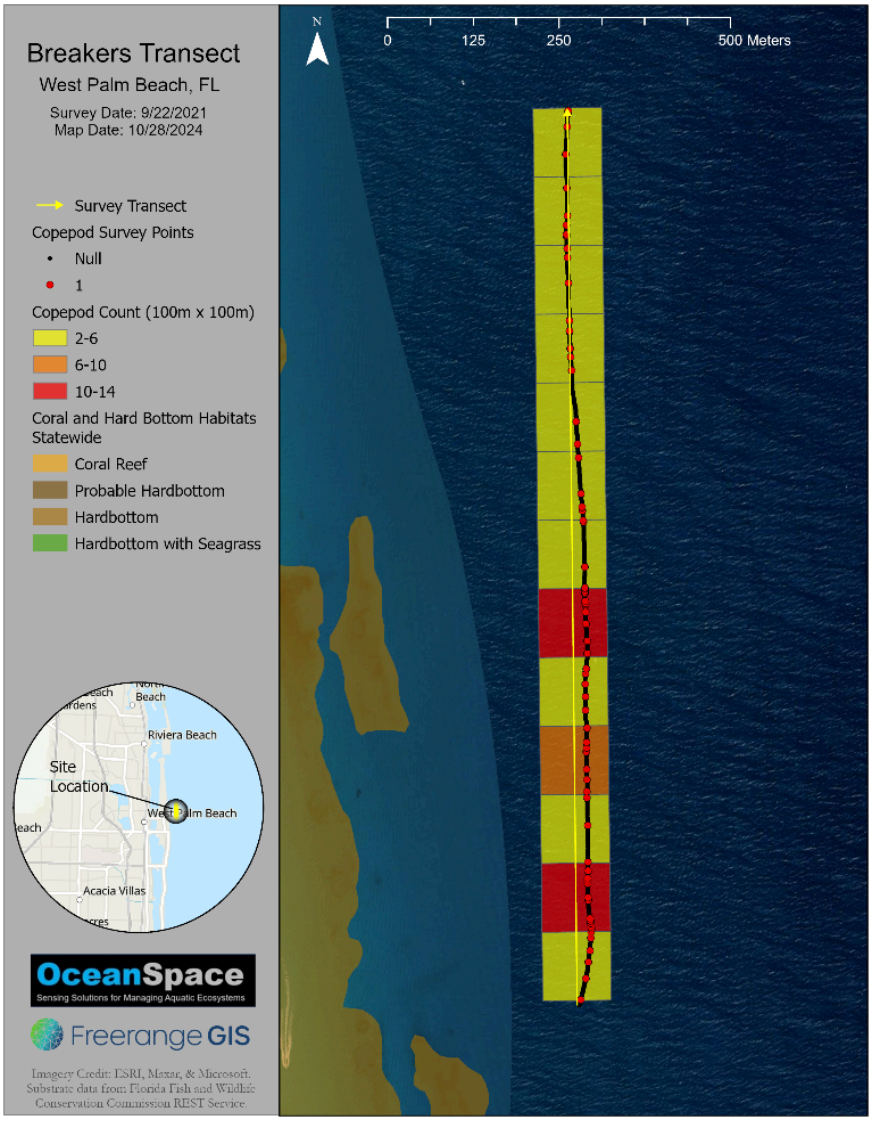

Figure 8. Plot of individual copepod occurrence along a sampling transect off the southeast coast of Florida, based on data collected by the Aquatic Imager using a sample collection methodology essentially identical to that used aboard the R/V Western Flyer.

Pairwise comparisons of plankton net samples vs Aquatic Imager samples collected from several locations in Tampa Bay reveal differences in outcomes (Appendix V). In visually sorted

and classified net samples, generally more taxa were identified relative to imaged samples. However, for those classes identified in both sample groups, in some instances (particularly copepods) a larger number of organisms were enumerated from the imaged samples. These results are somewhat preliminary, but they do support an expectation that outcomes will not be identical between net samples and imaged samples.

Questions specific to the Synchro testing effort include:

1. What was learned or achieved through this test deployment?

The imaging system exceeded expectations during the Western Flyer I deployment. Accuracy exceeding 90% following one training library expansion and reclassification was not anticipated. In other sample collection settings, such as Tampa Bay, Florida, 8-10 reclassifications have been required to achieve ~90% classification accuracy for individual taxon classes. As noted, the small number of classes obtained during the Monterey Bay cruise contributed to that rapid success.

2. Any significant failures/shortcomings and how they might be mitigated

A separate sampling event was conducted from the Santa Cruz pier, but that effort was replete with problems and complications, many of which resulted from sample delivery rather than system performance. Those difficulties included achieving a pump priming and water flowing through the imaging unit when we deployed the imaging unit in the work room, which was located ~7 m above the water intake. We solved that issue by deploying the pump and imager on a platform closer to the water intake (~ 1 m above), a solution that allowed sample collection but left the imager in a precarious position.

3. What are the next steps or phases of your progress?

Our focus at the present time is to refine our sample intake accessories, further develop the software and devise a scheme for serving from the cloud, and advance our marketing/sales efforts.

4. Connection with information users and use-cases.

    a. What information/knowledge do those data support?

        These data can provide high-resolution observations of zooplankton and other small particles that are important indicators of ecosystem productivity and food-web dynamics. For the California Current, information on the abundance and distribution of copepods, krill, decapods, pteropods, larval fish, and gelatinous zooplankton helps scientists understand changes in ocean conditions, forage availability for marine predators, and broader ecosystem responses to climate variability.

b. Who are the information users that will benefit from that knowledge?

   Primary users include researchers and monitoring programs such as ACCESS, universities, and ocean observing systems. Resource managers from NOAA, National Marine Sanctuaries, and fisheries management bodies can also use this data to support ecosystem assessments, wildlife conservation, and fisheries management. Additional users include environmental monitoring programs, educators, and the broader ocean science community.

c. Detail a potential data → information pipeline to reach society

   Data collected by the imaging system would be processed and classified to produce estimates of plankton abundance and distribution along survey transects. These data can then be integrated with environmental observations (temperature, salinity, oxygen) and incorporated into ecosystem monitoring programs and regional ocean observing systems. Synthesized results can inform ecosystem assessments, management decisions, and public reporting on ocean conditions through scientific publications, dashboards, and outreach products.

5. Take-home messages for information end-users and technology users

   The Aquatic Imager shows strong potential as a tool for rapidly observing plankton communities and other small particles in marine environments. Its ability to generate high-resolution imagery and near-real-time classifications could complement traditional plankton sampling methods and help expand monitoring coverage during ship surveys or fixed observing platforms. Continued testing across different environments and plankton communities will help determine how the system can best support long-term ecosystem monitoring and management applications.

Acknowledgements

Thanks to the captain and crew of the R/V Western Flyer for their responsive support.

References

Ali AK, Abdulhussein MA and Raheem SF (2023). Impact the classes' number on the convolutional neural networks performance for image classification. *International Journal of Advanced Science Computing and Engineering* 5(2): 119–128. doi.org/10.62527/ijasce.5.2.132

Bowman MN, McManamay RA, Rodriguez Perez A, Hamerly G, Arnold W, Steimle E, Kramer K, Norris B, Prangnell D and Matthews M (2024). Analysis of an optical imaging system prototype for autonomously monitoring zooplankton in an aquaculture facility. *Aqua. Eng.* 104. doi.org/10.1016/j.aquaeng.2023.102389.

Bowman MN, McManamay RA, Arnold W, Kramer K, Dean M, Prangnell D and Matthews M (2026). Optical imaging and machine learning to identify and enumerate early developmental stages of fish species. *Ecol. Inform.* 94. doi.org/10.1016/j.ecoinf.2026.103643

Hopcroft RR, Clarke C and Chavez FP (2002). Copepod communities in Monterey Bay during the 1997-1999 El Niño and La Niña. Prog. Oceanogr. 54: 251-264.

Karp MA, Peterson JO, Lynch PD, Griffis RB, Adams DF, Arnold WS and 20 others (2019). Accounting for shifting distributions and changing productivity in the development of scientific advice for fishery management. *ICES J. Mar. Sci.*, doi:10.1093/icesjms/fsz048.

Lombard F, Boss E, Waite AM, Vogt M, Uitz J, Stemmann L, Sosik HM, Schulz J, Romagnan J-B, Picheral M, Pearlman J, Ohman MD, Niehoff B, Möller KO, Miloslavich P, Lara-Lpez A, Kudela R, Lopes RM, Kiko R, Karp-Boss L, Jaffe JS, Iversen MH, Irisson J-O, Fennel K, Hauss H, Guidi L, Gorsky G, Giering SLC, Gaube P, Gallager S, Dubelaar G, Cowen RK, Carlotti F, Briseño-Avena C, Berline L, Benoit-Bird K, Bax N, Batten S, Ayata SD, Artigas LF and Appeltans W (2019). Globally consistent quantitative observations of planktonic ecosystems. *Front. Mar. Sci*. 6:196. doi: 10.3389/fmars.2019.00196.

NOAA (2025). 2024-25 California Current Ecosystem Status Report. doi.org/10.25923/9t48-pb48

Orenstein EC, Kenitz KM, Roberts PLD, Franks PJS Jaffe JS and Barton AD (2020). Semi- and fully supervised quantification techniques to improve population estimates from machine classifiers. *Limnol. Oceanogr.: Methods* 18: 739–753. doi: 10.1002/lom3.10399.

Palmer CP (2015). Marine biodiversity and ecosystems underpin a healthy planet and social well-being. *U.N. Chronicle 52 (2)*: 59-61.

Robinson KL, Sponaugle S, Luo JY, Gleiber MR and Cowen RK (2021). Big or small, patchy all: Resolution of marine plankton structure at micro- to submesoscales for 36 taxa. *Sci. Adv.* 7: eabk2904.

Rosa J, Batista LL and Monteiro-Ribas WM (2021). Spatio-temporal variability in the Cladocera assemblage of a subtropical hypersaline lagoon. Brazilian J. Biology 82: 1-9. doi: 10.1590/1519-6984.236354.

Appendix I: Western Flyer confusion matrix outcomes, with percentages (top) and numbers (bottom).

Reclassification Round 1:

Class_Name		Crustacea_Cladocera	Crustacea_Copepoda	Hemichordata_Chaetognatha	Detritus	Inanimate_Bubbles	Inanimate_Noise	NotKnown	SUM
Crustacea_Cladocera		13	10	0	1	0	4	0	28
Crustacea_Copepoda		0	41	0	0	0	11	0	52
Hemichordata_Chaetognatha		0	0	59	5	0	7	0	71
Detritus		0	2	2	371	3	10	0	388
									539
True Positive		13	41	59					
True Negative		511	475	466					
False Positive		15	11	12					
False Negative		0	12	2					
		539	539	539					
Accuracy		0.9097	0.8958	0.9115					
Precision		0.4643	0.7885	0.8310					
Recall		1.0000	0.7736	0.9672					
F1		0.6341	0.7810	0.8939					
Specificity		0.9715	0.9774	0.9749					

Reclassification Round 2:

Class_Name		Crustacea_Cladocera	Crustacea_Copepoda	Hemichordata_Chaetognatha	Detritus	Inanimate_Bubbles	Inanimate_Noise	NotKnown	SUM
Crustacea_Cladocera		39	2	0	1	1	1	1	45
Crustacea_Copepoda		4	99	1	0	0	6	2	112
Hemichordata_Chaetognatha		2	0	142	3	0	2	1	150
Detritus		0	0	0	0	0	0	0	0
									307
True Positive		39	99	142					
True Negative		256	193	156					
False Positive		6	13	8					
False Negative		6	2	1					
		307	307	307					
Accuracy		0.9609	0.9511	0.9707					
Precision		0.8667	0.8839	0.9467					
Recall		0.8667	0.9802	0.9930					
F1		0.8667	0.9296	0.9693					
Specificity		0.9771	0.9369	0.9512					

Reclassification Round 3:

Class_Name		Crustacea_Cladocera	Crustacea_Copepoda	Hemichordata_Chaetognatha	Detritus	Inanimate_Bubbles	Inanimate_Noise	NotKnown	SUM
Crustacea_Cladocera		64	3	0	1	0	0	2	70
Crustacea_Copepoda		5	183	1	0	1	7	2	199
Hemichordata_Chaetognatha		3	0	180	3	0	0	2	188
Detritus		0	0	0	0	0	0	0	0
									457
True Positive		64	183	180					
True Negative		379	255	268					
False Positive		6	16	8					
False Negative		8	3	1					
		457	457	457					
Accuracy		0.9694	0.9584	0.9803					
Precision		0.9143	0.9196	0.9574					
Recall		0.8889	0.9839	0.9945					
F1		0.9014	0.9506	0.9756					
Specificity		0.9844	0.9410	0.9710					

Reclassification Round 4:

Class_Name		Crustacea_Cladocera	Crustacea_Copepoda	Hemichordata_Chaetognatha	Detritus	Inanimate_Bubbles	Inanimate_Noise	NotKnown	SUM
Crustacea_Cladocera		64	3	0	2	0	3	4	76
Crustacea_Copepoda		5	183	2	0	4	5	11	210
Hemichordata_Chaetognatha		4	0	181	3	0	1	11	200
Detritus		49	60	29	375	3	26	16	558
									1044
True Positive		64	183	181					
True Negative		910	771	813					
False Positive		12	27	19					
False Negative		58	63	31					
		1044	1044	1044					
Accuracy		0.9330	0.9138	0.9521					
Precision		0.8421	0.8714	0.9050					
Recall		0.5246	0.7439	0.8538					
F1		0.6465	0.8026	0.8786					
Specificity		0.9870	0.9662	0.9772					

Reclassification Round 5:

Class_Name		Crustacea_Cladocera	Crustacea_Copepoda	Hemichordata_Chaetognatha	Detritus	Inanimate_Bubbles	Inanimate_Noise	NotKnown	SUM
Crustacea_Cladocera		79	4	0	1	0	3	4	91
Crustacea_Copepoda		6	204	2	1	1	6	10	230
Hemichordata_Chaetognatha		3	1	202	3	0	1	10	220
Detritus		54	60	32	378	4	13	18	559
									1100
True Positive		79	204	202					
True Negative		946	805	846					
False Positive		12	26	18					
False Negative		63	65	34					
		1100	1100	1100					
Accuracy		0.9318	0.9173	0.9527					
Precision		0.8681	0.8870	0.9182					
Recall		0.5563	0.7584	0.8559					
F1		0.6781	0.8176	0.8860					
Specificity		0.9875	0.9687	0.9792					

Reclassification Round 6:

Class_Name		Crustacea_Cladocera	Crustacea_Copepoda	Hemichordata_Chaetognatha	Detritus	Inanimate_Bubbles	Inanimate_Noise	NotKnown	SUM
Crustacea_Cladocera		79	4	0	1	0	3	4	91
Crustacea_Copepoda		6	204	2	1	1	6	10	230
Hemichordata_Chaetognatha		3	1	202	3	0	1	10	220
Detritus		54	60	32	378	4	13	18	559
									1100
True Positive		79	204	202					
True Negative		946	805	846					
False Positive		12	26	18					
False Negative		63	65	34					
		1100	1100	1100					
Accuracy		0.9318	0.9173	0.9527					
Precision		0.8681	0.8870	0.9182					
Recall		0.5563	0.7584	0.8559					
F1		0.6781	0.8176	0.8860					
Specificity		0.9875	0.9687	0.9792					

Reclassification Round 7:

Class_Name		Crustacea_Cladocera	Crustacea_Copepoda	Hemichordata_Chaetognatha	Detritus	Inanimate_Bubbles	Inanimate_Noise	NotKnown	SUM
Crustacea_Cladocera		93	0	1	0	0	2	10	106
Crustacea_Copepoda		3	220	1	0	1	0	7	232
Hemichordata_Chaetognatha		0	0	219	1	0	0	18	238
Detritus		0	0	0	0	0	0	0	0
									576
True Positive		93	220	219					
True Negative		467	344	336					
False Positive		13	12	19					
False Negative		3	0	2					
		576	576	576					
Accuracy		0.9722	0.9792	0.9635					
Precision		0.8774	0.9483	0.9202					
Recall		0.9688	1.0000	0.9910					
F1		0.9208	0.9735	0.9542					
Specificity		0.9729	0.9663	0.9465					

Appendix II: Exemplary images collected by the Aquatic Imager during the November 12, 2024, sampling cruise aboard the R/V Western Flyer. Top row were classified as cladocerans, middle row as copepods, and bottom row as chaetognaths. Note that images are enlarged, which results in some blurring. Increments are 1 mm.

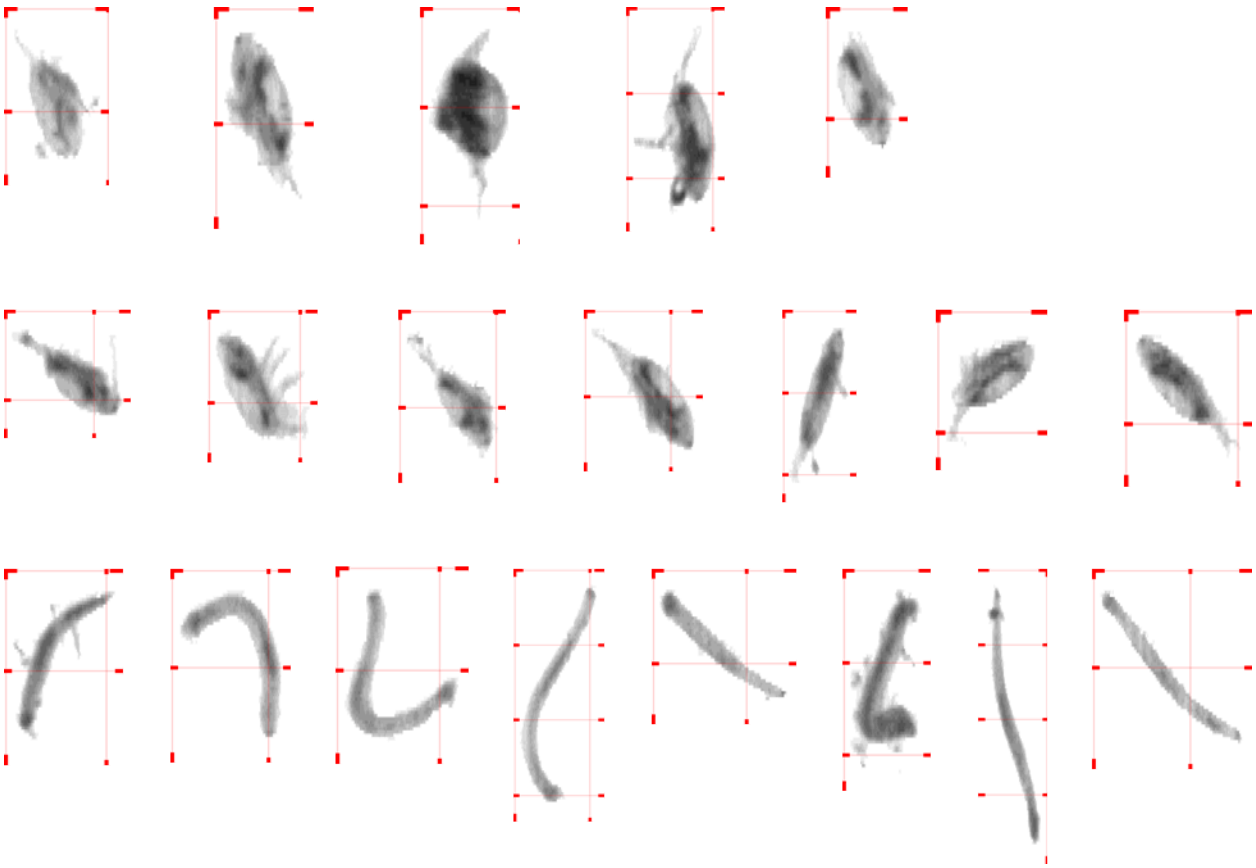

Appendix III: Exemplary images obtained by the Aquatic Imager from net-based samples collected using a Tucker Trawl arrangement with 335 micron mesh aboard the R/V Weatherbird.

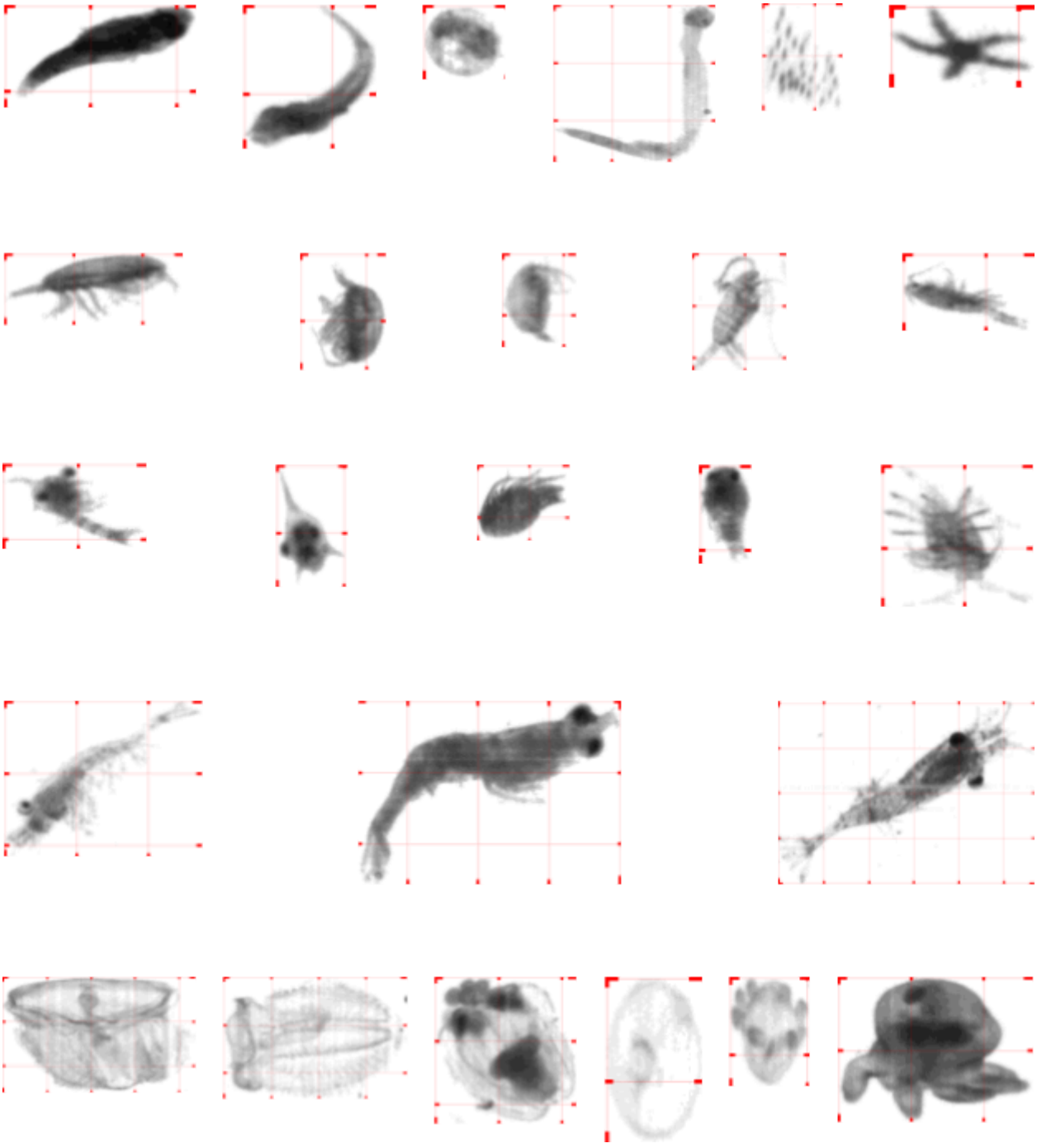

Appendix IV: Classification accuracy analysis for several organism classes sampled from Tampa Bay, Florida.

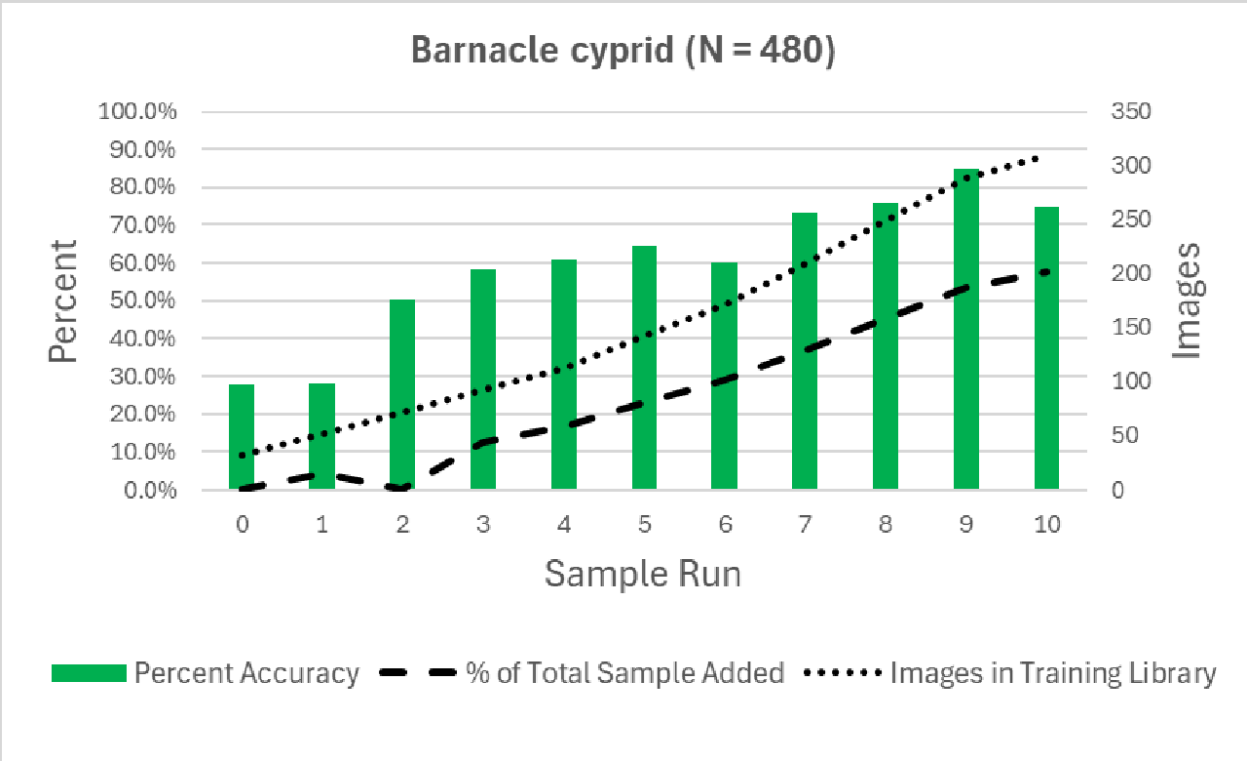

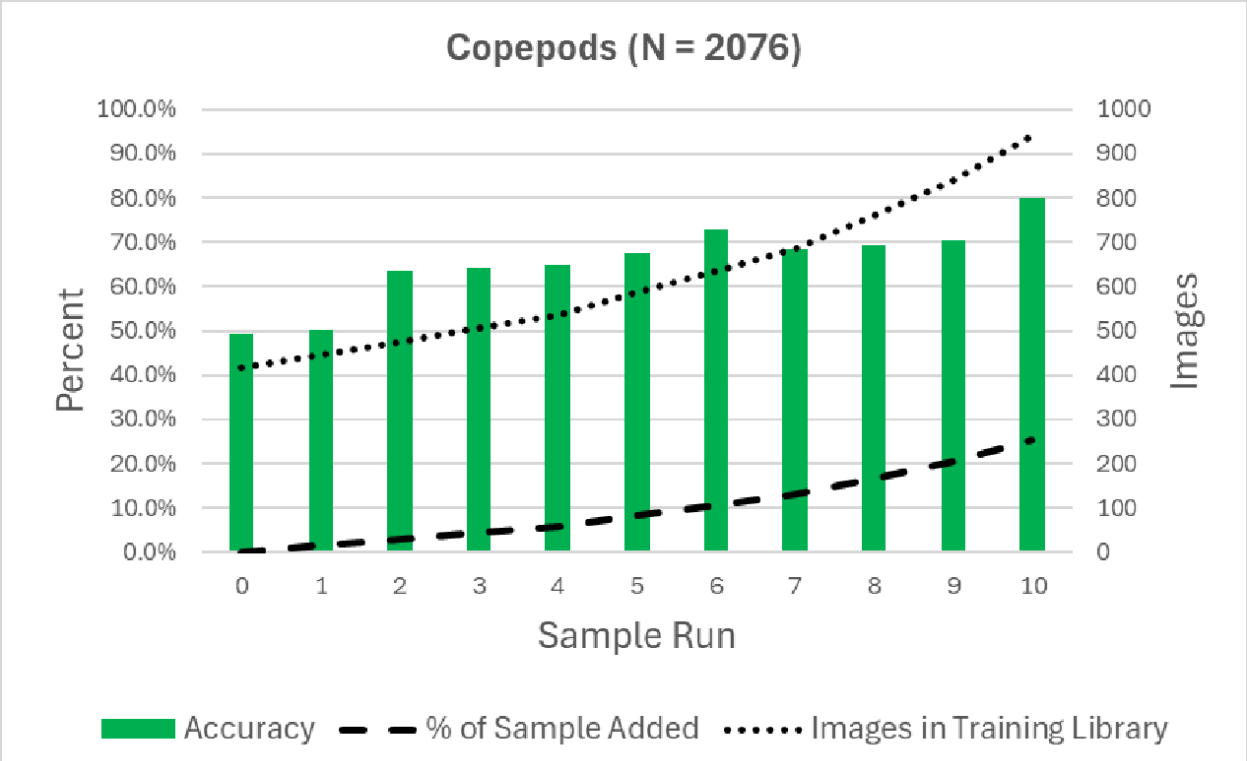

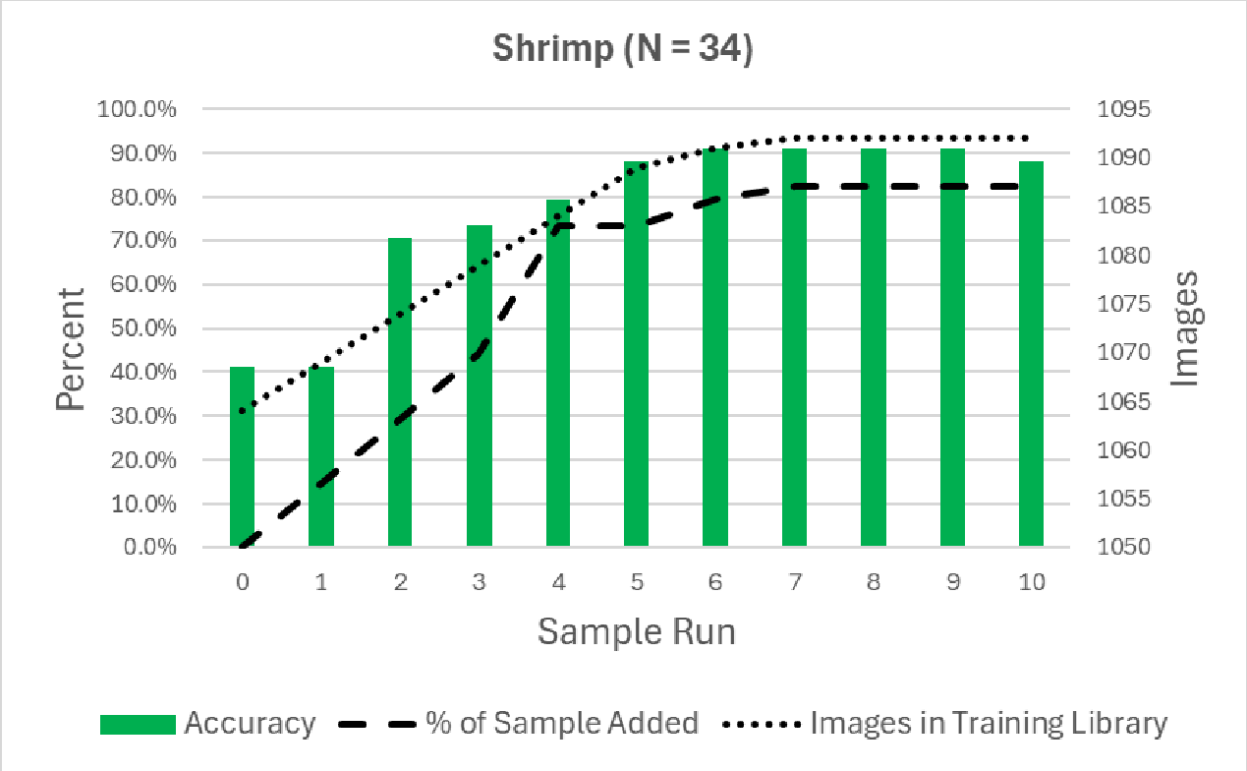
Shrimp (N = 34)
100.0%
90.0%
80.0%
70.0%
60.0%
50.0%
40.0%
30.0%
20.0%
10.0%
0.0%
Percent
1095
1090
1085
1080
1075
1070
1065
1060
1055
1050
Images
0 1 2 3 4 5 6 7 8 9 10
Sample Run
Accuracy
% of Sample Added
Images in Training Library

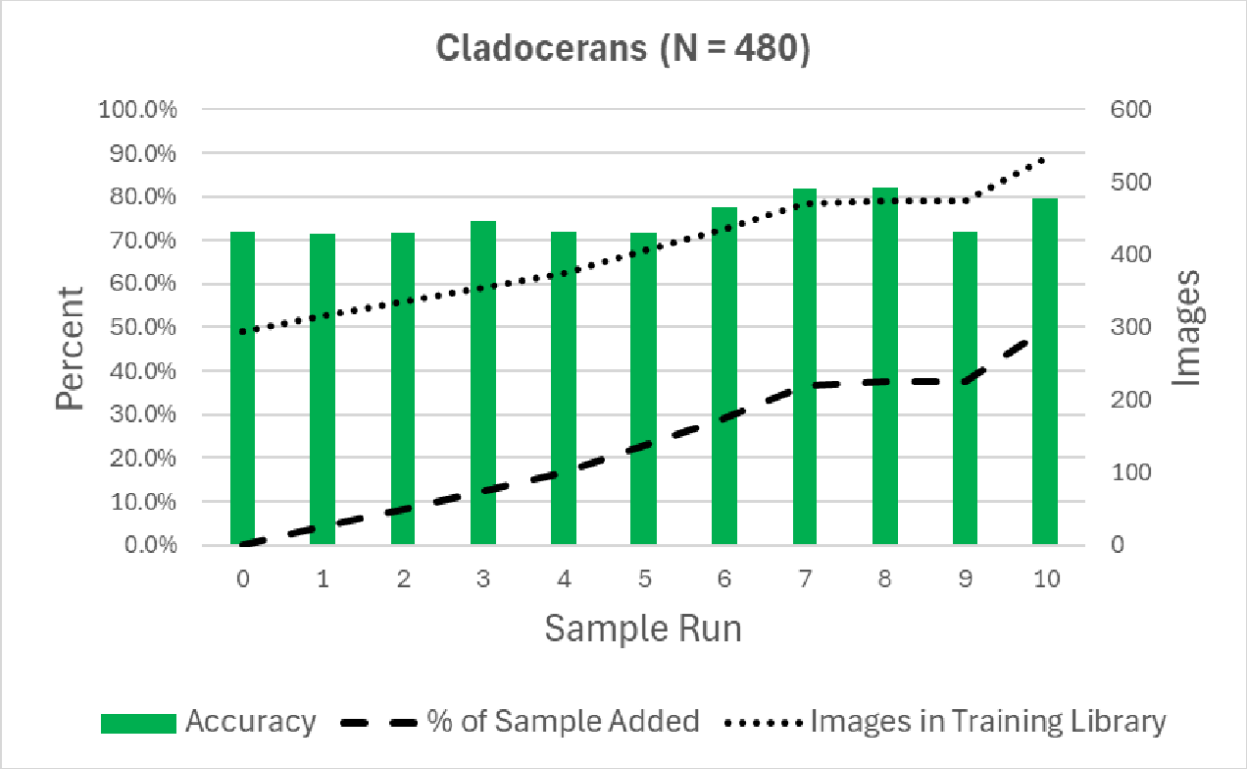
Cladocerans (N = 480)
100.0%
90.0%
80.0%
70.0%
60.0%
50.0%
40.0%
30.0%
20.0%
10.0%
0.0%
Percent
600
500
400
300
200
100
0
Images
0 1 2 3 4 5 6 7 8 9 10
Sample Run
Accuracy
% of Sample Added
Images in Training Library

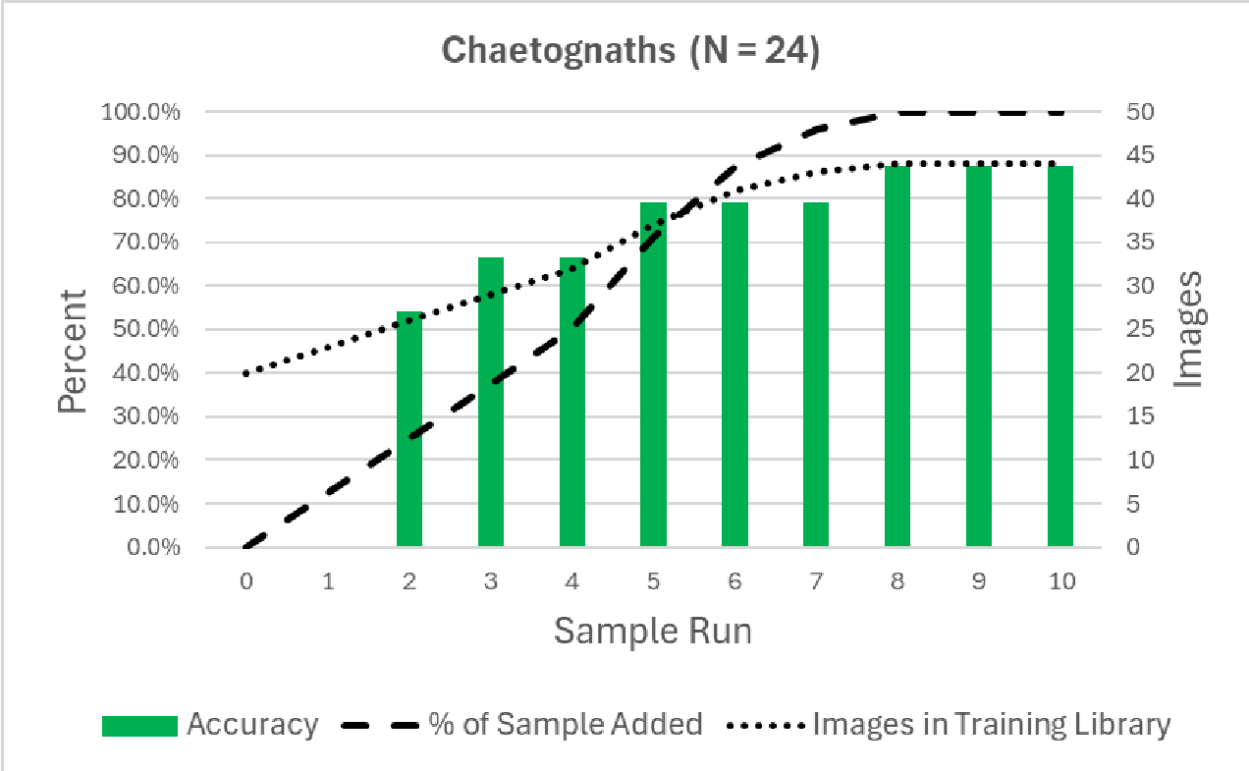
Chaetognaths (N = 24)
Percent
100.0%
90.0%
80.0%
70.0%
60.0%
50.0%
40.0%
30.0%
20.0%
10.0%
0.0%
Images
50
45
40
35
30
25
20
15
10
5
0
0 1 2 3 4 5 6 7 8 9 10
Sample Run
Accuracy
% of Sample Added
Images in Training Library

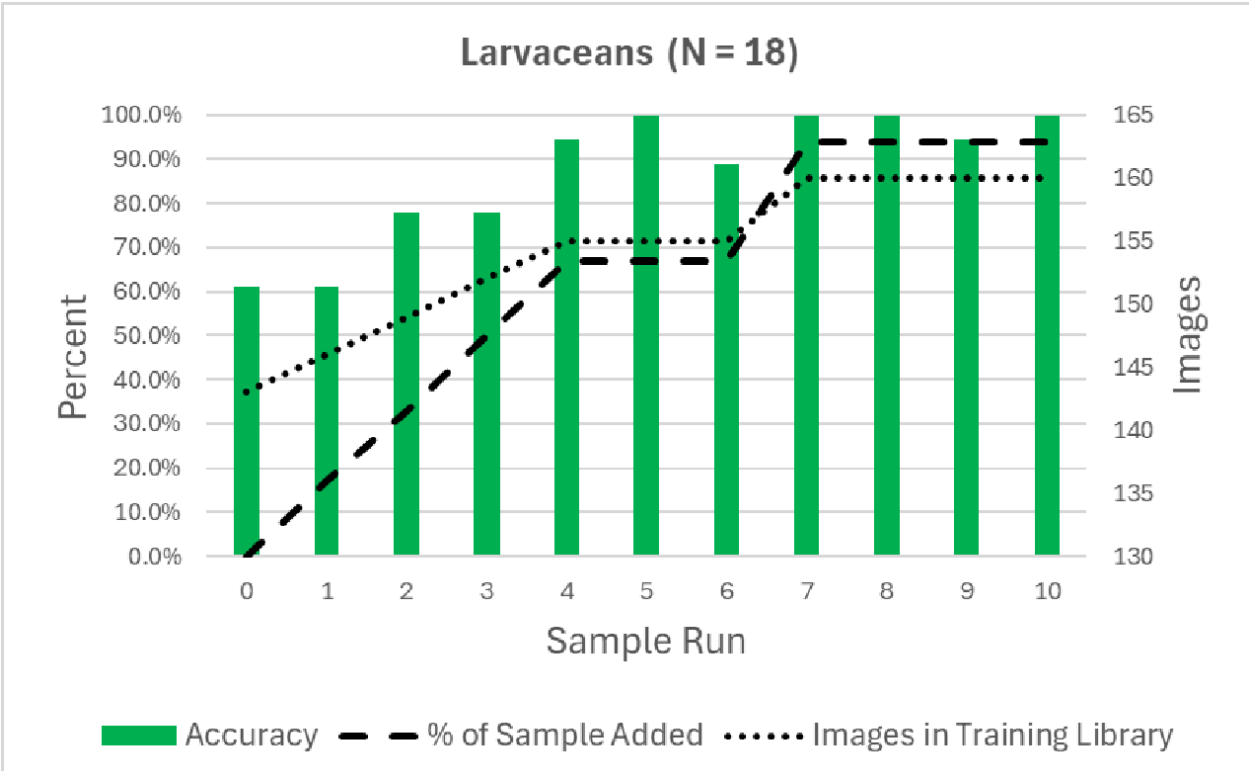
Larvaceans (N = 18)
Percent
100.0%
90.0%
80.0%
70.0%
60.0%
50.0%
40.0%
30.0%
20.0%
10.0%
0.0%
Images
165
160
155
150
145
140
135
130
0 1 2 3 4 5 6 7 8 9 10
Sample Run
Accuracy
% of Sample Added
Images in Training Library

Appendix V: Results from pairwise comparison of net collected samples visually analyzed by taxonomic experts versus sample classifications provided by the Aquatic Imager.

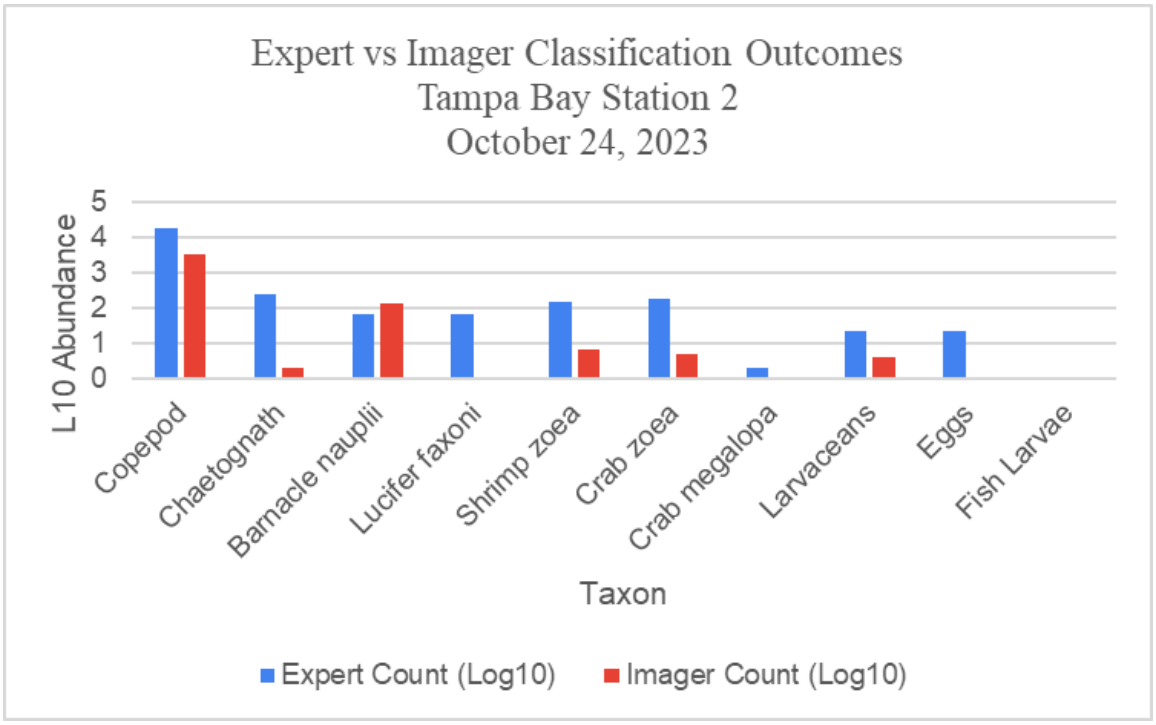

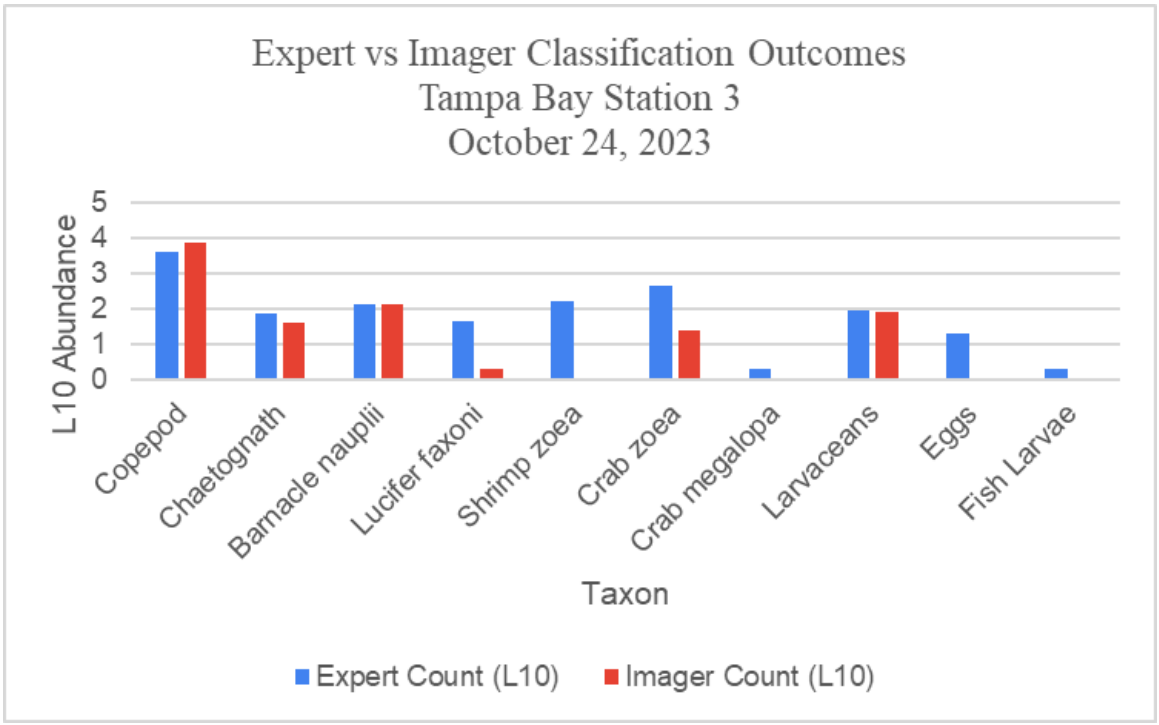

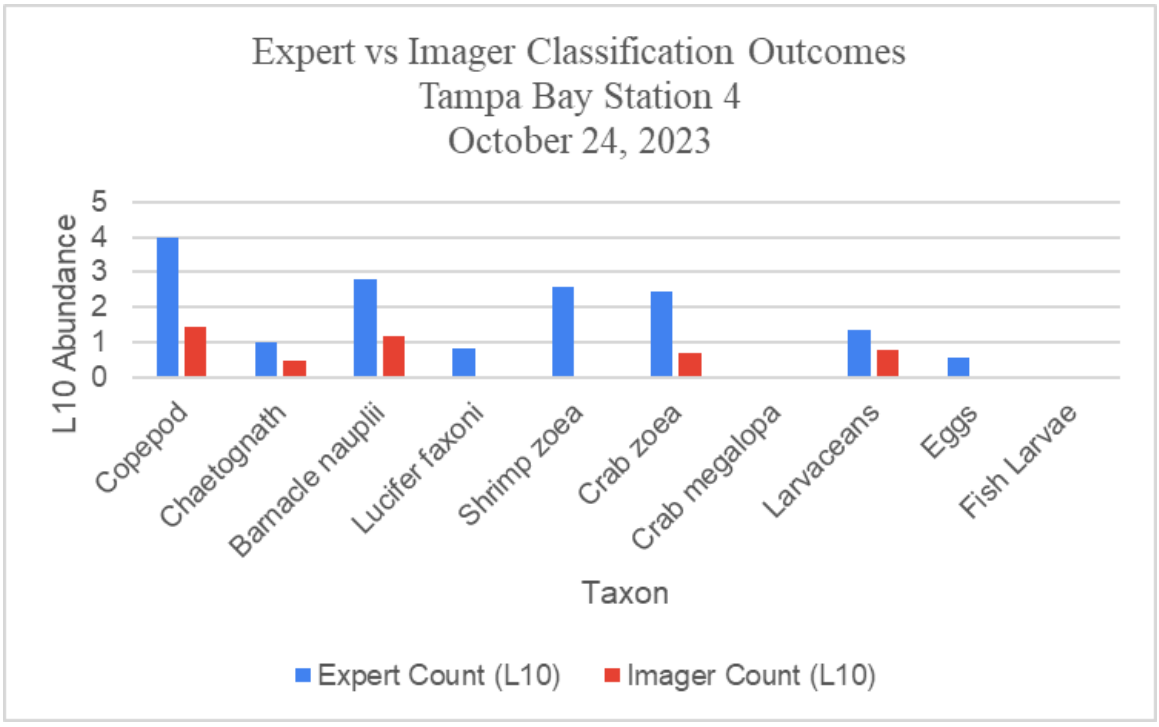
Expert vs Imager Classification Outcomes
Tampa Bay Station 4
October 24, 2023
L10 Abundance
5
4
3
2
1
0
Copepod
Chaetognath
Barnacle nauplii
Lucifer faxoni
Shrimp zoea
Crab zoea
Crab megalopa
Larvaceans
Eggs
Fish Larvae
Taxon
Expert Count (L10)
Imager Count (L10)

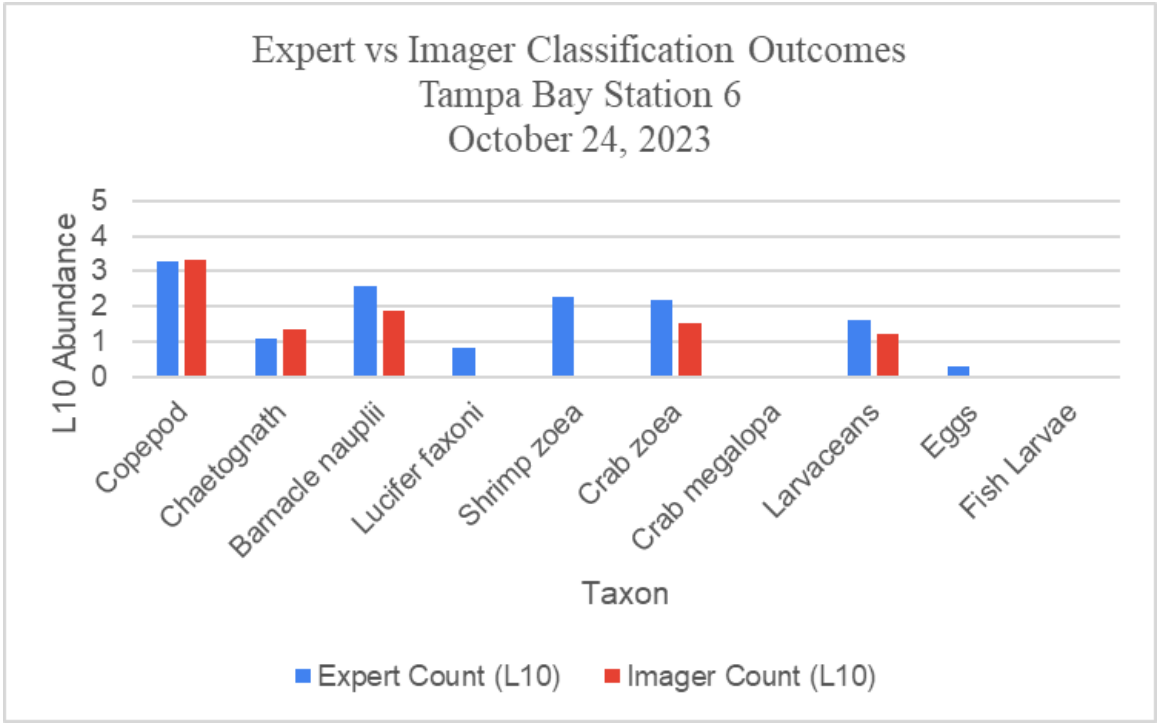
Expert vs Imager Classification Outcomes
Tampa Bay Station 6
October 24, 2023
L10 Abundance
5
4
3
2
1
0
Copepod
Chaetognath
Barnacle nauplii
Lucifer faxoni
Shrimp zoea
Crab zoea
Crab megalopa
Larvaceans
Eggs
Fish Larvae
Taxon
Expert Count (L10)
Imager Count (L10)

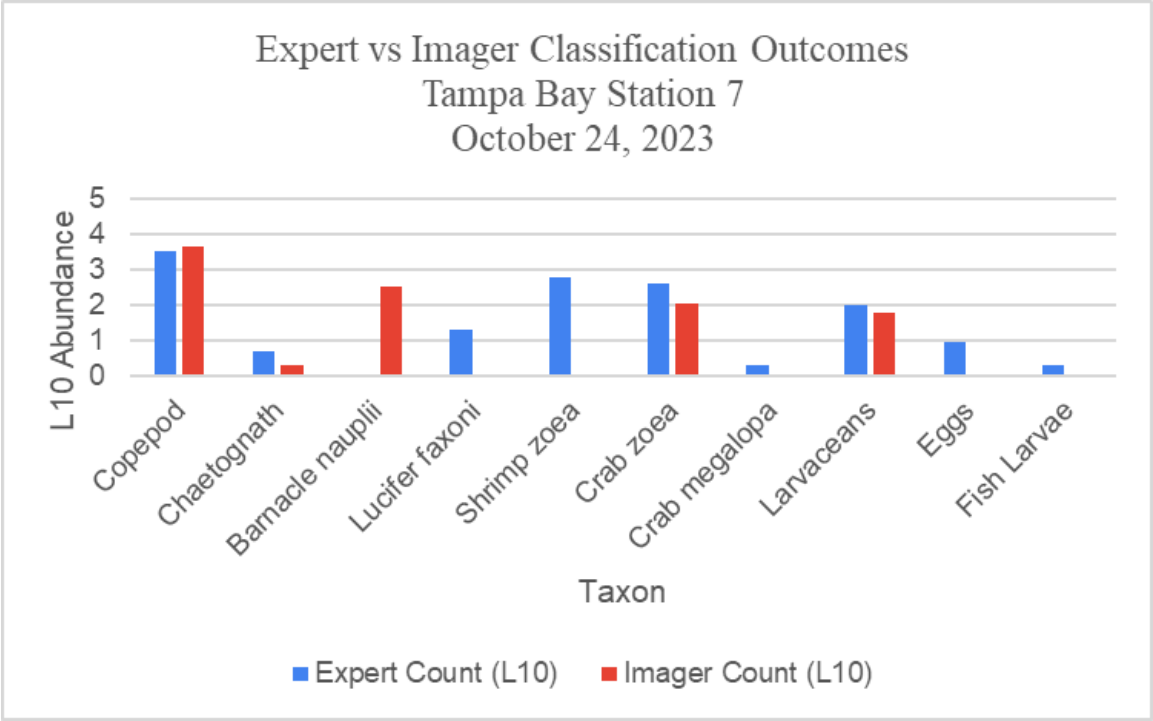
Expert vs Imager Classification Outcomes
Tampa Bay Station 7
October 24, 2023
L10 Abundance
5
4
3
2
1
0
Copepod
Chaetognath
Barnacle nauplii
Lucifer faxoni
Shrimp zoea
Crab zoea
Crab megalopa
Larvaceans
Eggs
Fish Larvae
Taxon
Expert Count (L10)
Imager Count (L10)

Cover Photo by OceanSpace LLC

Synchro accelerates the adoption of innovative ocean observation technologies by providing no-cost access to evaluation platforms like research vessels, buoys, and seawater pump stations.

info@oceansynchro.io | www.oceansynchro.io

Access Providers

CENTRAL & NORTHERN CALIFORNIA OCEAN OBSERVING SYSTEM

Monterey Bay Aquarium Research Institute

Axiom DATA SCIENCE A TETRA TECH COMPANY

UC SANTA CRUZ

UNIVERSITY of WASHINGTON

SJSU SAN JOSÉ STATE UNIVERSITY

Stanford | Doerr School of Sustainability Oceans

Stanford Center for Ocean Solutions

Hakai Science on the Coastal Margin

Moss Landing Marine Laboratories

Synchro's Sponsors

GORDON AND BETTY MOORE FOUNDATION

Schmidt Marine TECHNOLOGY PARTNERS

oceankind